LA-UR-22-21422

Approved for public release; distribution is unlimited.

Title:	Small Mammal Prey Study for the Mexican Spotted Owl at Two Locations at Los Alamos National Laboratory
Author(s):	Velardi, Milu Sue Gadek, Chauncey Ryland
Intended for:	Report
Issued:	2022-02-18

LA-UR-22-xxxxx
February 2022

Small Mammal Prey Study for the Mexican Spotted Owl at Two Locations at Los Alamos National Laboratory

Chauncey R. Gadek and Milu S. Velardi

Los Alamos
NATIONAL LABORATORY

Prepared for: U.S. Department of Energy/National Nuclear Security Administration
Los Alamos Field Office

Prepared by: **Chauncey R. Gadek**
Milu S. Velardi
Environmental Protection and Compliance Division
Resources Management Team
Los Alamos National Laboratory

Editing and Layout by: **Hannah Conrad**
Communication Arts and Services

CONTENTS

Figures

Contents

Tables

1 EXECUTIVE SUMMARY

In New Mexico, Mexican spotted owls *(Strix occidentalis lucida*) are typically found in rocky canyons consisting of mixed-conifer forests that have experienced minimal human disturbance. At Los Alamos National Laboratory (LANL), Mexican spotted owls have been found breeding and foraging in habitats consistent with their known biology, but face the impact of human encroachment in the surrounding upland habitat. Little is known about the prey base present within the Laboratory's vast forests. In anticipation of expanding human development in proximity to known occupied owl habitat, the goal of our study was to evaluate the small mammal prey base available to Mexican spotted owls at the Laboratory and to assess prey availability, diversity and composition.

We sampled two study plots within the Laboratory's forests for small mammals in 2021. Study plots were situated in conifer, deciduous, mixed conifer-deciduous and mixed oak. Our small mammal trapping efforts and SCR modeling revealed site-specific differences in prey base diversity, abundance and density between the unoccupied Pajarito Canyon and nearby occupied Mortandad Canyon site. These results highlight how managing tracts of land for small mammal prey base may overlap with goals set forth by researchers for Mexican spotted owl habitat needs. We recommend further trapping efforts to better understand prey availability in occupied and unoccupied sites at LANL as well as further investigation of prey selection through the dissection of pellets found in the areas surrounding known nesting locations.

2 INTRODUCTION

The Mexican spotted owl (*Strix occidentalis lucida*) is a forest- and canyon-dwelling owl in the southwestern United States and northern Mexico (Gutierrez et al. 2020), and has been listed as a threatened species since 1993 (USFWS 1995, 2012). The Mexican spotted owl has the largest geographic range of the three subspecies. The range extends from the southern Rocky Mountains in Colorado and the Colorado Plateau in southern Utah southward through Arizona and New Mexico and discontinuously through the Sierra Madre Occidental and Oriental to the mountains at the southern end of the Mexican Plateau (USFWS 1995, 2012).

Mexican spotted owls nest, forage, roost and disperse in a wide variety of biotic communities. Mixed-conifer forests are commonly used throughout the range and may include Douglas fir (*Pseudotsuga menziesii*), white fir (*Abies concolor*), southwestern white pine (Pinus strobiformis), limber pine (*Pinus flexilis*) and ponderosa pine (*Pinus ponderosa*). Understory may include Gambel oak (*Quercus gambelii*), maples (*Acer spp.*), boxelder (*Acer negundo*) and New Mexico locust (*Robinia neomexicanus*). The highest densities of Mexican spotted owls occur in mixed-conifer forests that have experienced minimal human disturbance. At LANL, Mexican spotted owls have been identified in these rocky canyon habitats – consisting of steep cliffs and narrow canyons of primarily tall mixed-conifer species.

Within the boundaries of LANL, little is known about the prey base of nesting Mexican spotted owls. We designed a study to better understand the small mammal prey base present within the designated core habitat near an active nest site. Core habitat is defined as specific areas of habitat essential for the long-term survival of listed species. This research seeks to determine if there was a difference in small mammal populations between occupied and unoccupied habitats. Our objectives were to: (1) quantify and compare the small mammal prey base available near an active nest site in Mortandad Canyon and in an equivalent habitat in adjacent Pajarito Canyon that is not occupied and (2) determine if small mammal capture rates vary between the two sites.

By documenting the availability and abundance of various small mammal species present in LANL, we will gain a better understanding of dietary choice available to nesting and foraging owls in northern New Mexico and be able to make more informed, site-specific management recommendations. We quantify small mammal communities by sampling them using a live trapping method and applying spatial capture recapture (SCR) models (Royle et al. 2014) to estimate relative small mammal densities between a site known to be occupied and one unoccupied by Mexican spotted owls (LANL 2021).

3 MATERIALS AND METHODS

3.1 Study Area

LANL and the associated residential areas of Los Alamos and White Rock are located in Los Alamos County in north-central New Mexico, approximately 95 km (60 mi) north-northeast of Albuquerque and 40 km (25 mi) northwest of Santa Fe. The 103.6 km^2 (25,600-acre) LANL site is situated on the Pajarito Plateau.

3.2 Selection of Study Plots

Small mammal trapping was conducted in the Pajarito and Mortandad Canyons in areas designated as core habitat by the LANL Habitat Management Plan (LANL 2017). The Pajarito Canyon (Pajarito) (Figure 1) transect grid was selected due to its proximity to the Mortandad Canyon sampling site, having a similar habitat and being an unoccupied core habitat for the owl. Pajarito is located approximately 1.5 km (0.9 mi) south-southwest from a known nest location in Mortandad Canyon. In 2000, following the Cerro Grande wildfire, a large concrete flood retention structure was built directly in this canyon bottom to mitigate for runoff upstream, following the Cerro Grande wildfire. The sampling location was selected upstream from this structure in habitat unaffected by the construction of the structure. The area sampled for this study consisted of mixed-conifer woodlands, primarily ponderosa pine, Douglas fir, Gambel oak, coyote willow (*Salix exigua*), bluestem willow (*Saliz irrorata*), poison ivy (*Oxicodendron radicans*), Wood's rose (*Rosa woodsia*) and New Mexico hops (*Humulus lupulus var. neomexicanus*). Soils in the area are well drained but supported a diverse community of forbs and grasses with a somewhat incised channel running through the middle of the entire study area.

The Mortandad Canyon (Mortandad) transect grid is located on an elevated bench above the canyon bottom. Mortandad bench is located north approximately 1.4 km (0.85 mi) north-northeast of the Parajito trapping site. It was selected for its close proximity (adjacent) to the nest. This area is dominated by ponderosa pine, Douglas fir, southwestern white pine, mountain mahogany (*Cerocarpus ledifolius*) and Gambel oak (Figure 2). Understory was less dense and shrubs were less prevalent than in Pajarito and the ground in most areas consisted of a rockier substrate than Pajarito Canyon. The ground surface in this study site consisted of mostly weathered rocky outcrops with shallow rooted vegetation scattered throughout intermittent pockets of well-drained soil. This site did have a fairly high amount of coarse woody debris throughout. Mexican spotted owls have been documented in Mortandad Canyon since 2013 (LANL 2021).

Figure 1. Pajarito trapping at Los Alamos National Laboratory.

Figure 2. Mortandad trapping site at Los Alamos National Laboratory.

3.3 Small Mammal Trapping

We live trapped small mammals from June 6 to August 1 in 2021 (baseline year of study). We established four plot lines evenly distributed (10 m apart) throughout both study areas, each consisting of 25 traps spaced in 10 m intervals. One medium Sherman live traps (7.5 × 9.5 × 9.5 cm) (H.B. Sherman Traps, Inc., Tallahassee, Florida) was placed at each grid point (100 traps at each study area total). We baited traps with a mix of corn, oats and barley coated with molasses combined with peanut butter and provided cotton for bedding. We set traps in the evening (1800–2000 hrs) and checked traps in the morning (0700–0800 hrs) for 10 days at each site. Traps were closed during the day to decrease the possibility of imposing heat stress and avoid bycatch of non-target species. All trap locations in the grid were recorded with a Trimble GPS unit.

All analyses were completed in the R statistical programming language using the R studio interface (R Development Core Team 2021; Rstudio Team 2021). We used trap detections of unique individuals as a proxy for abundance as well as models to estimate density and population size. Species richness was

determined from trapping data summaries. To assess species diversity from trap detections, we used the R package *vegan* (Oksanen et al. 2020) to calculate the Shannon diversity index (Shannon 1948) of each trapping site. We ran Chi-square tests to determine if sex ratios differed significantly from a null expectation of 1:1 (males: females) or 1:1 (adults:(juveniles + sub adults)).

We fit maximum likelihood SCR models for each trapping site in the R statistical software package *secr* v4.4.7 (Efford 2021) to estimate the density and population size of the Mexican woodrat (*Neotoma mexicana*) and the brush mouse (*Peromyscus boylii*) for Mortandad Canyon only, due to sparse detections at the Pajarito site for these species. Additionally, since several other species were infrequently captured that represent relevant Mexican spotted owl prey items (Ganey 1992; Seamans and Gutierrez 1999; Block et al. 2005; LANL 2006; Willey 2013), we separately modeled pooled small mammal detections for each site. We captured individual animals in single-catch live-traps, a trap configuration for which no current likelihood estimator is available. However, Efford et al. (2009) found that, as long as per bout trap usage remained low (< 86% trap saturation), single-catch traps modeled as multi-catch produced unbiased density estimates. Trap saturation (the number of occupied traps per trapping occasion) at both sites remained well below this threshold, (Mortandad: 8.4 ± 1.6%; Pajarito: 2.5 ± 1.3%; Appendix Figure A-1) allowing us to use a multinomial observation model to model traps as multi-catch (Royle et al. 2014).

Depending on the species and/or site, initial model selection indicated both a negative exponential and a half-normal detection function which best described the decreasing probability of capturing an individual with increasing distance between a trap and the animal's activity center for our data (Royle et al. 2014; Efford 2021) (Appendix Table A-1). Models estimate the two free parameters of the half-normal and negative exponential detection functions: the detection probability of an individual at its activity center (g_0), and the spatial detection scale (σ), which demonstrates the rate of declining detection probability with distance from a trap (Borchers and Efford 2008; Royle et al. 2014), as well as the density per hectare of the species being modeled. After initial exploration of detection function distance decay, we delineated buffers around traps based on likelihood estimation of sigma for each dataset. The buffers define the state space across which our models estimate detection probability, spatial scale of movement and density (Appendix Figures A-2 through A-5). These conservative buffers, $\geq 4*\sigma$, ensure the probability of not detecting an animal near the edge of our defined state space is nearly zero.

Detection probability (g_0) and spatial scale of detection (σ) can be influenced by an individual animal's proclivity to avoid or seek out traps (Otis et al. 1978). For example, baited traps have been known to increase the likelihood of animals visiting them (du Preez et al. 2014). To account for these learned responses in our density estimates, we modeled a general behavioral response model (g_0 *and/or* $\sigma \sim b$) and a trap-specific (g_0 *and/or* $\sigma \sim bk$) model where animals are drawn to or avoid specific traps. Additional variation in g_0 and σ can arise when different groups in a population (sex, age, etc.) behave differently. To assess whether demographic or unknown groupings influenced parameter estimates, we modeled the likelihood that g_0 and/or σ varied by sex (g_0 *and/or* $\sigma \sim$ Sex), coarse age category (i.e., juvenile, sub adult, adult; g_0 *and/or* $\sigma \sim$ Age) and latent classes not explained by sex or age with two-class finite mixture models (g_0 *and/or* σ h2).

SCR models operate under the default assumption that animals inhabit circular home ranges and detection probability attenuates radially away from an animal's activity center (Borchers and Efford 2008). However, landscape features may bias movement patterns, distorting assumed home range geometry. Because our trapping sites were aligned with the orientation of a narrow canyon and on a narrow bench (Appendix Figures A-2 through A-5), we used model selection by AIC_C to determine if our trapping data supported the use of an anisotropic transformation of the detection function (Murphy et al. 2016) (Appendix Table A-1 through Table A-2). This spatial transformation accounts for the possibility that animal movement was biased in the orientation of the canyon, effectively elongating individual home

ranges. We obtained angles of orientation for Pajarito Canyon (107°) and Mortandad (103°) trapping grids to perform the anisotropic transformation with the custom function adapted from Murphey et al. (2016) using the R package *geoR* (Ribeiro and Diggle 2020).

We compared our per-species per-site sets of models using AIC corrected for small sample size (AIC_C) (Burnham and Anderson 2004; Burnham et al. 2011). We reported density estimates, detection probability (g_0), and the spatial detection scale (σ) for the highest ranked models by AIC_C within two units of one another. We then extrapolated local per-site population size estimates ($\widehat{N}$) by multiplying the per-hectare density, $\widehat{D}$, estimates by the total habitat mask over which the likelihood surface was modeled.

4 RESULTS

4.1 Site Abundance, Richness, and Diversity

We recorded 84 encounters at the Mortandad site while recording only 25 at the Pajarito site during each of the 10-day trapping bouts. Individual recaptures ranged from 0-7 among both sites. For detailed encounter history information for each site see Appendix Figures A-6 through A-10. Among the 109 total encounters, we captured a total of 41 unique individuals encompassing five different species during a total of 20 trap nights during the baseline year of 2021 (Table 1). Mexican woodrats were the most abundant small mammals captured across both sites (n = 23), accounting for 56% of all captures. The brush mouse was the second most captured mammal at 34% (n = 14), followed by the western harvest mouse (*Reithrodontomys megalotis*) at 5% (n = 2). The remaining species captured (all = 5%) were plains harvest mouse (*Reithrodontomys montanus*) (Figure 3) and deer mouse (*Peromyscus maniculatus*) (Figure 3). Species richness was slightly higher in Pajarito (n = 4) than Mortandad trapping sites (n = 3) (Table 1). Shannon diveristy was low for both sites but marginally higher at the Pajarito trapping site ($H = 0.78$) relative to the Mortandad trapping site ($H = 0.73$).

Table 1. Number of unique small mammal captures by trapping grid from 2021 trapping season. Data was collected over the summer of 2021 at LANL in Los Alamos County, New Mexico.

Latin Name	Common Name	Pajarito	Mortandad	Total
Neotoma mexicana	Mexican woodrat	8	15	23
Reithrodontomys megalotis	Western harvest mouse	2	0	2
Peromyscus boylii	Brush mouse	1	13	14
Reithrodontomys montanus	Plains harvest mouse	1	0	1
Peromyscus maniculatus	Deer mouse	0	1	1
Total		**12**	**29**	**41**

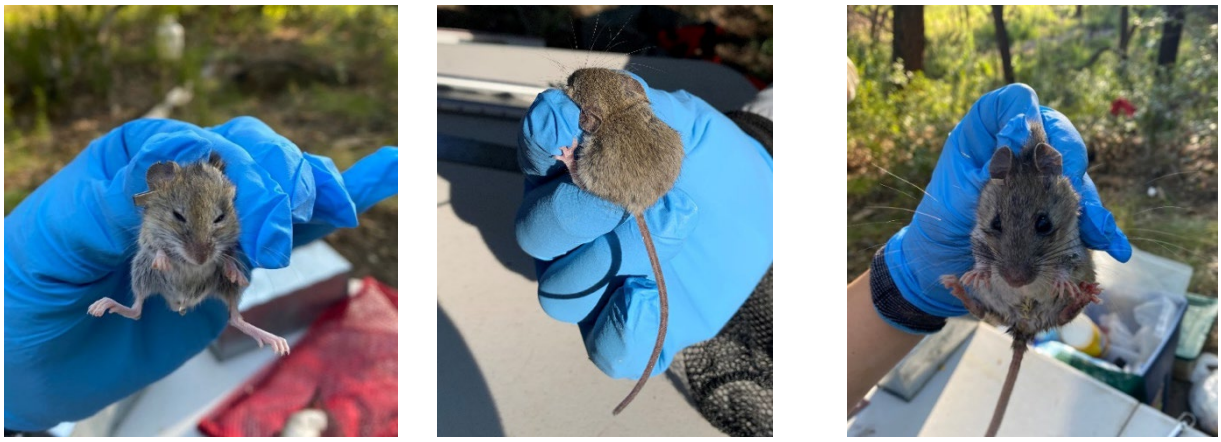

Figure 3. Examples of individual species captured at LANL. Western harvest mouse (left), plains harvest mouse (middle) captured at Pajarito, and deer mouse (right) captured at Mortandad. Note dorsal stripe on plains harvest mouse in middle photo.

4.2 Demographics

Among all species and sites, both sexes were equivalently encountered (χ^2 (2, N = 109) = 0.2, P = 0.7). The Mexican woodrat sex ratio at Mortandad was 23:25 (males to females) (χ^2 (2, N = 49) = 0.1, P = 0.8) while at Pajarito the ratio was 5:4 (χ^2 (2, N = 19) = 0.5, P = 0.5). The brush mouse sex ratio at Mortandad was 8:9 (χ^2 (2, N = 34) = 0.1, P = 0.7). Age structure was weighted towards adult woodrats at the Mortandad site with ~35% of individuals classified as sub-adult or juvenile (χ^2 (2, N = 49) = 4.6, P = 0.03). The Mexican woodrat at Pajarito and brush mouse at Mortandad were evenly represented in age structure between adult and young individuals (Pajarito Mexican woodrat: χ^2 (2, N = 19) = 0.1, P = 0.8); Mortandad brush mouse: χ^2 (2, N = 34) = 1.0, P = 0.3).

4.3 Animal Movement

Distances between successive trapping encounters showed variability between species and sites (Figure 3) with Mexican woodrat at Mortandad moving a median 10.3 meters (IQR = 13.8) while Mexican woodrat at the Pajarito site moved a median 17.2 meters (IQR = 54.4). The brush mouse at Mortandad moved a median 19.0 meters (IQR = 19.9) (Figure 4).

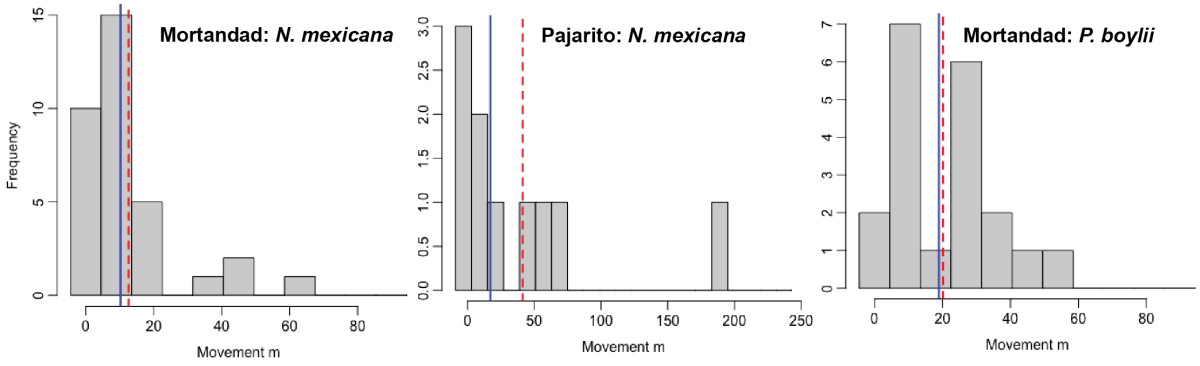

Figure 4. Successive movements in meters of Mexican woodrat at Mortandad and Pajarito sites and brush mouse at Mortandad trapping site. Blue solid line represents median movement distance while red dashed line represents mean movement distance.

4.4 Density and Population Size Estimates from SCR Models

Because sample sizes for the Western harvest mouse, Plains harvest mouse and Deer mouse were all ≤ 2, and they are less likely high-value prey items for Mexican spotted owls, we divided our modeling results into species-sites combinations with the greatest encounter numbers and pooled total small mammal captures. A negative exponential detection function was highest ranked by AIC_C during initial model selection for all species-site combinations (Appendix Table A-1). An anisotropic transformation of the detection function was supported as ranked by AIC_C for the Mexican woodrat ($\Phi = 1.43$, 95% CI = 0.5-3.8; Appendix Table A-1 & Appendix Figure A-11) and for the brush mouse in Mortandad ($\Phi = 1.9$, 95% CI = 0.8-4.7; Appendix Table A-1 & Appendix Figure A-12). The anisotropic transformation was not supported for the Mexican woodrat in Pajarito, likely due to sparse encounter data penalizing models with additional parameters ($\Delta AIC_C = 10.5$) (Appendix Table A-1). Model selection supported an anisotropic transformation for both sites when pooling all small mammal data (Appendix Table A-2 & Appendix Figure A-13 and Figure A-14).

Detection probability (g_0) varying with a positive trap-specific behavioral response (bk), reflecting animals seeking out traps after an initial encounter, was supported in the top model for the Mexican woodrat in Mortandad (Table 2 & Table 3). The top model for the Mexican woodrat in Mortandad estimated density at 9.2 individuals/ha (95% CI = 5.2 – 16) (Table 2). Extrapolating the density across the total area of the modeled state space (3.81 ha) we estimated the population size for the Mexican woodrat at the Mortandad trapping site to be $\widehat{N} = 36$ individuals (95% CI = 21 – 64) (Figure 5). The top model for the Mexican woodrat at the Pajarito site was an isotropic model holding all parameters constant (Table 2 & Table 3). The density estimate from the top model for the Mexican woodrat at the Pajarito site was significantly lower ($t = 4.7$, $P < 0.0001$) at 1.06 individuals/ha (95% CI = 0.38 – 2.93) placing population estimates at $\widehat{N} = 4$ individuals (95% CI = 1–11) across the same 3.81 ha state space, though the modeled state space for Pajarito was considerably larger (19 ha). The top model for the brush mouse at Mortandad site included an anisotropically transformed detection function and held all parameters constant (Table 2). The density estimate for brush mouse at the Mortandad site was 7.47 individuals/ha (95% CI = 4.15 – 13.4) (Table 2) extrapolating across the modeled state space to a local population size of at $\widehat{N} = 28$ individuals (95% CI = 16 – 51) (Figure 5). AIC_C ranked two top models equivalently for the pooled species detection models at both the Mortandad site ($\Delta AIC_C = 1.9$; Table 2) and Pajarito site ($\Delta AIC_C = 1.9$; Table 2). The top models for Mortandad small mammal density both included a trap-specific behavior response term (bk) (Table 2 & Table 3), suggesting animals tended to revisit the baited traps after initial detection. One of the top models also included sex as a covariate for detection probability (g_0) (Table 2 & Table 3), indicating a marginally higher likelihood of capturing female animals. Similarly, one of the top models for the pooled small mammal detections at the Pajarito site included the bk response term (Table 2). Estimates for pooled small mammal densities and by extension population size mirrored those of the Mexican woodrat density estimates, with Mortandad estimated to have significantly higher ($t = 4.4$, $P < 0.0001$) density and population size estimates than estimates from the Pajarito canyon grid (Table 2 & Figure 6).

Table 2. Estimates of detection probability (g0), spatial scale (σ), and density ($\hat{D}$) for top models for each species and/or site combination model set. Estimates from multiple equivalent top models are averaged. Separate estimates are reported for sex grouping covariate (female (F); male (M)) when they varied by more than 0.001 units. 95% confidence intervals are reported in parentheses.

Mortandad			
Mexican woodrat			
Highest ranked Model(s)	g_0	σ	$\hat{D}$
$D(\sim1)\ g_0(\sim bk)\ \sigma(\sim1)\ \Phi(\sim1)$	0.13 (0.01–0.61)	5.6 (2.2–14)	9.2 (5.2–16)
$D(\sim1)\ g_0(\sim bk + sex)\ \sigma(\sim1)\ \Phi(\sim1)$			
$D(\sim1)\ g_0(\sim1)\ \sigma(\sim1)\ \Phi(\sim1)$			
Brush mouse			
Highest ranked Model(s)	g_0	σ	$\hat{D}$
$D(\sim1)\ g_0(\sim1)\ \sigma(\sim1)\ \Phi(\sim1)$	0.05 (0.03–0.08)	8.6 (5.5–14)	7.5 (4.1–13)
Pajarito			
Mexican woodrat			
Highest ranked Model(s)	g_0	σ	$\hat{D}$
$D(\sim1)\ g_0(\sim1)\ \sigma(\sim1)$	0.01 (0.01–0.04)	50 (29–88)	1.1 (0.4–2.9)
Mortandad			
Pooled small mammal species			
Highest ranked Model(s)	g_0	σ	$\hat{D}$
$D(\sim1)\ g_0(\sim bk)\ \sigma(\sim1)\ \Phi(\sim1)$	F: 0.14 (0.07–0.26)	4.8 (3.3–6.9)	17 (11–26)
$D(\sim1)\ g_0(\sim bk + sex)\ \sigma(\sim1)\ \Phi(\sim1)$	M: 0.12 (0.07–0.22)		
Pajarito			
Pooled small mammal species			
Highest ranked Model(s)	g_0	σ	$\hat{D}$
$D(\sim1)\ g_0(\sim bk)\ \sigma(\sim1)\ \Phi(\sim1)$	0.03 (0.01–0.12)	8.6 (3.2–23)	5.1 (2.1–13)
$D(\sim1)\ g_0(\sim1)\ \sigma(\sim1)\ \Phi(\sim1)$			

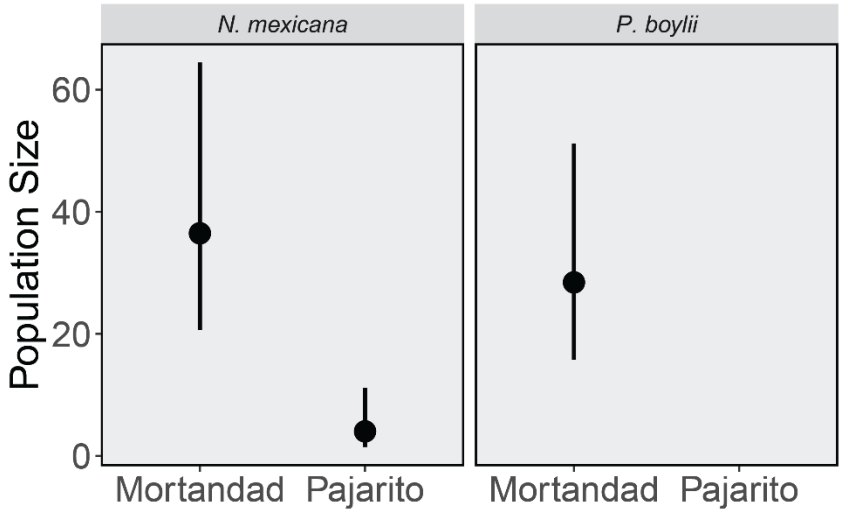

Figure 5. Population size estimates and 95% CI extrapolated across 4.51 hectares to control for trapping site size differences from top models selected by AIC_C for the Mexican woodrat (left panel) at both sites and the brush mouse at Mortandad site (right panel).

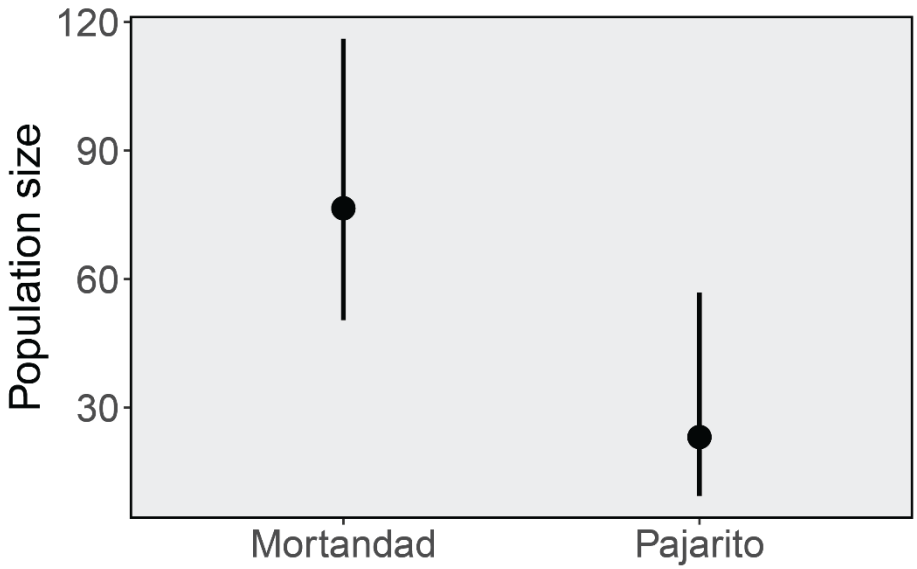

Figure 6. Population size estimates and 95% CI extrapolated across 4.51 hectares to control for state space size differences between sites from top models selected by AIC_C for small mammals at both sites.

Table 3. Top five models for each species and/or site with adequate encounter data or pooled across all species ranked by Akaikes Information Criterion corrected for small sample size (AIC_C). Models estimated D (density in individuals per hectare), detection probability (g_0), spatial scale of detection (σ), and angle of home range elongation (Φ). g_0 and σ parameters were allowed to be constant (~1), or vary by sex (~sex), trap specific (bk) and un-specific (b) learned responses, unspecified two class latent mixtures (π), and combination thereof. Table reports number of parameters (K), AIC adjusted for small sample sizes (AIC_C), relative differences between model and highest ranked model AIC_C (ΔAIC_C), model weight (ω), and log likelihood of model (logLik).

Mortandad					
Mexican woodrat					
Model	K	AIC_C	ΔAIC_C	ω	logLik
D(~1) g_0(~bk) σ(~1) Φ(~1)	6	441.8	0.0	0.96	–209.7
D(~1) g_0(~bk + sex) σ (~1) Φ(~1)	7	449.3	7.5	0.02	–209.7
D(~1) g_0(~1) σ (~1) Φ(~1)	5	450.0	8.2	0.02	–216.7
D(~1) g_0(~1) σ (~bk + sex) Φ(~1)	7	453.2	11	0.00	–211.6
D(~1) g_0(~1) σ (~sex) Φ(~1)	6	455.0	13	0.00	–216.2
Brush mouse					
Model	K	AIC_C	ΔAIC_C	ω	logLik
D(~1) g_0(~1) σ (~1) Φ(~1)	5	391.1	0.0	0.66	–186.8
D(~1) g_0(~bk) σ (~1) Φ(~1)	6	393.8	2.7	0.17	–184.9
D(~1) g_0(~sex) σ (~1) Φ(~1)	6	394.7	3.6	0.11	–185.3
D(~1) g_0(~1) σ (~sex) Φ(~1)	6	397.4	6.3	0.03	–186.7
D(~1) g_0(~b) σ (~1) Φ(~1)	6	397.4	6.3	0.03	–186.7
Pajarito					
Mexican woodrat					
Model	K	AIC_C	ΔAIC_C	ω	logLik
D(~1) g_0(~1) σ (~1)	4	253.7	0.0	0.91	–116.2
D(~1) g_0(~bk) σ (~1)	5	258.3	4.6	0.10	–109.2
D(~1) g_0(~1) σ (~sex)	5	271.1	17	0.00	–115.6
D(~1) g_0(~sex) σ (~1)	5	271.1	17	0.00	–115.6
D(~1) g_0(~b) σ (~1)	5	271.8	18	0.00	–115.9
Mortandad					
Pooled small mammal species					
Model	K	AIC_C	ΔAIC_C	ω	logLik
D(~1) g_0(~bk) σ (~1) Φ(~1)	6	785.1	0.0	0.64	–384.6
D(~1) g_0(~bk + sex) σ (~1) Φ(~1)	7	787.0	1.9	0.22	–383.8
D(~1) g_0(~bk + sex) σ (~sex) Φ(~1)	8	789.4	4.3	0.08	–383.1
D(~1) g_0(~sex) σ (~bk + sex) Φ(~1)	8	792.4	7.3	0.02	–384.6
D(~1) g_0(~bk + sex) σ (~bk + sex) Φ(~1)	9	793.3	8.2	0.01	–382.9
Pajarito					
Pooled small mammal species					
Model	K	AIC_C	ΔAIC_C	ω	logLik
D(~1) g_0(~bk) σ (~1) Φ(~1)	6	310.9	0.0	0.72	–141.0
D(~1) g_0(~1) σ (~1) Φ(~1)	5	312.8	1.9	0.27	–146.4
D(~1) g_0(~1) σ (~sex) Φ(~1)	6	320.6	9.8	0.01	–145.9
D(~1) g_0(~sex) σ (~1) Φ(~1)	6	320.7	9.9	0.01	–146.0
D(~1) g_0(~b) σ (~1) Φ(~1)	6	321.5	11	0.00	–146.4

5 DISCUSSION

We conducted two trapping bouts at sites occupied (Mortandad) and unoccupied (Pajarito) by the Mexican spotted owl to address our two objectives of quantifying and comparing the spotted owl's small mammal prey base between sites and determining if capture rates varied by site. Broadly, we found communities of nearly equivalent richness and diversity, but dissimilar capture rates led to differences in density estimates between sites. Below, we discuss factors potentially driving these differences and the management implications for LANL's Mexican spotted owls, while placing our results within the context of similar small mammal studies from the southwest and locally at LANL.

SCR modeling revealed site-specific differences in prey base abundance and density between the unoccupied Pajarito and nearby occupied Mortandad site. Between sites we captured four of 12 species in the rodent family (*Muridae*) known to occur at LANL and the surrounding areas (LANL 1997). We identified one individual as a plains harvest mouse, a species not formerly documented at LANL, from the Pajarito trapping site, which had marginally higher species richness than the Mortandad site (Table 1). Diversity indices were low compared with previously calculated indices from Mortandad and Sandia Canyons (LANL 2005), with both sites being dominated by Mexican woodrats. In 2005, LANL biologists' Mortandad trapping sites were dominated by deer mice and they captured several long-tailed voles (*Microtus longicaudus*) and vagrant shrew species (*Sorex vagrans*). These differences in small mammal community composition are most likely attributable to habitat differences and trap types between studies. LANL 2005 trapped in the more mesic Mortandad Canyon bottom compared to the more xeric conditions at the Mortandad trapping site in 2021. The 2005 study also used pitfall traps which can potentially capture and retain a wider diversity of small mammal species (Caceres et al. 2011). However, the distance between the more mesic canyon bottom and bench in the present study is less than 30 meters (100 ft) and well within the likely home range size of a Mexican woodrat (Cranford 1977; Lindstedt et al. 1986; Lynch et al. 1994). Elevated encounters at the Mortandad relative to Pajarito suggest higher local abundances, though the degree to which site-specific habitat differences, timing of trapping bouts and other unrecorded variables may affect relative abundances remains unknown. We captured nearly twice the number of unique Mexican woodrat individuals and 13 times the number of unique brush mouse individuals at Mortandad versus Pajarito (Table 1), both of which represent likely prey items for the Mexican spotted owl across its range (Ganey 1992; Seamans and Gutierrez 1999; Block et al. 2005; Willey 2013). Local dietary composition analyses from pellet collection confirms that LANL Mexican spotted owls rely heavily on woodrat and *Peromyscus* species (LANL 2006).

Broadly, the demographics of sites were equivalent or lacked a clear pattern. Among all species combined, sex ratios were approximately 1:1 at both sites. Age classes showed no clear pattern between species and sites, though we would expect age structure to vary between species and fluctuate throughout the year depending on species-specific timing of breeding. Differences in age structure between sites for small mammals could be due to site and time-specific factors influencing detection probabilities. For example, trapping later in the year could increase the ratio of identified adults versus juveniles for some species depending on the timing of breeding intervals, as individuals lose diagnostic juvenile characteristics and younger animals often exhibit higher mortality rates (Caughley 1966). Because of the high mortality rates of r-selected small mammal species, like the deer mouse, a sampling duration of 14-30 days is recommended (Dupont et al. 2019) for optimally accurate and precise estimates from SCR models. Therefore, our 10-day sampling periods may have prevented us from building an optimal dataset to robustly estimate density of the brush mouse.

SCR models revealed significant differences in density and, by extension, population size of the Mexican woodrat between trapping sites. Models produced substantially higher density estimates for the Mortandad relative to Pajarito trapping site (Figure 6 & Table 2). Our results are not entirely in line with estimates from more primitive density calculation methods that neglected spatial heterogeneity and

detection probability. For example, Cranford (1982) estimated woodrat and deer mouse abundance in California, though in different species from our own, by dividing the number of individuals by the trapping area finding an order of magnitude higher density of deer mice (~40 individuals/ha) to our highest estimate and woodrat density (~10.2 individuals/ha) nearly equivalent to our Mortandad estimate. Interestingly, Cranford (1982) found strong correlations between the presence of dusky-footed woodrat (*Neotoma fuscipes*) nests and the abundance of the pinyon mouse (*Peromyscus truei*), suggesting a similar positive feedback mechanism could be operating in Mortandad Canyon. In 2005, LANL biologists captured the majority of Mexican woodrats and brush mice together at the same trapping sites in Mortandad Canyon (LANL 2005). Though facilitation between species is a compelling explanation, an equivalently likely explanation of site-specific density differences are the overall more favorable conditions at the Mortandad site due to its proximity to water.

More sophisticated spatially explicit capture-recapture methods from related species in New Mexico have generated density estimates in line with ours. Enclosures of deer mouse species at the Sevilleta National Wildlife Refuge in central New Mexico contained true densities of 3.27—6.29 individuals/ha from which estimated densities for a larger small mammal community using SCR models were strongly correlated (Gerber and Parmenter 2015). More recently, Gaukler et al. 2020 estimated a combined deer mouse species density in neighboring Sandia Canyon to be nearly a third of our density estimate for the brush mouse in Mortandad Canyon. Our deer mouse detections from Pajarito were too sparse to adequately model, suggesting low densities and substantial variability across LANL. Historical small mammal sampling at LANL, though unable to produce density estimates, hints at similar variability finding differing species compositions and detection numbers within canyon systems (LANL 2005). These previous studies situate our estimates amid a highly variable prey landscape for the Mexican spotted owl. Only a small portion of two of LANL's six Mexican spotted owl Areas of Environmental Interest (AEI) are covered in the present study. Further data collection is needed to complete our understanding of the highly variable distribution of prey species across spotted owl AEIs at LANL.

We found substantially higher capture rates at the occupied Mortandad site relative to the unoccupied Pajarito site. Capture rates are directly related to the extent of animal movement across the trapping area. Differences in body size between species and habitat types between trapping sites create expectations about movement differences. For example, larger species like the Mexican woodrat may be expected to travel further than smaller mammal species like the brush mouse based on expectations of home range size and dispersal distances (Cranford 1977; Lindstedt et al. 1986; Vernes 2003). Similarly, differences between trapping site habitats and topography may effect animal movement (Vernes 2003). However, trapping data revealed no clear differences in movement distances of animals between sites (Figure 4). More data are needed to determine if site-specific movement patterns exist or are the result of noise rising above our small sample sizes. Additionally, ambient light conditions may effect animal movement patterns (Jensen and Honess 1995; Yunger et al. 2002; Hoffmann et al. 2019). Though our trapping bouts occurred during both waxing and waning phases of the moon cycle given their semi-continuous operation, lack of experimental design to capture moonlight effects, and sparse encounter rates, we were unable to model variation in trapping histories and nighttime ambient light conditions. Artificial light from neighboring developed areas may affect local prey bases and impact foraging success of the Mexican spotted owl. Extensions of this study could benefit from designing trapping bouts to capture both low and high ambient light conditions between sites and potentially introducing artificial light sources to examine the effects on animal detection probability and movement patterns.

The Mortandad trapping site was located along a bench in Mortandad Canyon on a hard rocky substrate lacking vegetation relative to the Pajarito Canyon site which was located in a narrow canyon bottom. The differences in elevation and vegetation cover may affect many factors (e.g., ambient light levels, food sources distribution, etc.) leading to downstream differences in detection probability between sites. For example, if food is scarce, detection probability may increase as animals travel farther to forage and

would likely respond more positively to baited traps. Proximity to foraging sites could be an explanation for the high relative densities estimated for Mortandad relative to Pajarito trapping sites, though we did not measure, map nor model the distribution of food sources across the trapping sites.

Though tempting to ascribe differences in small mammal capture rates and density estimates to the preferential nest site selection of Mexican spotted owls (Ward et al. 1998), we lack the replication and sample sizes necessary to draw definitive conclusions connecting prey base to Mexican spotted owl occupancy. More broadly, we find that the prey base in both canyons seem healthy relative to other similar studies (Block et al. 2005; Ganey et al. 2014). Our efforts help establish a baseline for the local Mexican spotted owl available prey populations. Continued trapping efforts across different sites and times of year will ensure model estimates are as robust as possible to assess occupied and unoccupied habitat and to inform sound management decisions for the species.

6 RECOMMENDATIONS FOR MANAGEMENT

We recommend continued investigations of prey species present in Mexican spotted owl habitat at LANL, as dietary preferences vary widely across regions (Ward and Block 1995) and likely impact recovery and stability of populations. Because the degree to which site-specific habitat differences, timing of trapping bouts, and other unrecorded variables may affect relative abundances remains unknown, LANL biologists recommend continued trapping bouts to allow for replication with inclusion of additional explanatory factors, including ground vegetation, overstory composition, ambient light levels and climatic changes (drought, temperature, etc.). Management strategies that maintain suitable habitat and prey bases (e.g., forest with elements or characteristics of mature forest structure) should receive high conservation priority.

In addition to current and future surveys at these sites, it would be beneficial to gain a better understanding of the direct dietary choices of nesting owls found at LANL. Past and ongoing collection and forthcoming analysis of pellets can be compared against modeled densities of small mammals from this study. Because little is known about the diets of owls in this region of northern New Mexico, LANL biologists are in a unique position to connect decades of continuing occupancy data with growing estimates of prey diversity and abundance. These data will help further our understanding of the Mexican spotted owl's foraging landscape and how it may influence nest site selection, improving management of the species.

7 ACKNOWLEDGMENTS

We would like to acknowledge Sean Murphy for his advisement on SCR modeling. We would also like to acknowledge Jesse Berryhill and Jessica Johnson for their handling and measuring of small mammals and for providing expertise in the field. For managing trap deployment, baiting and assisting with animal handling, we would like to thank Elisa Abeyta and Jadzia Rodriguez. And finally, we would like to thank Chuck Hathcock for his guidance in establishing this study and for getting the mice in a line.

8 LITERATURE CITED

Block, W.M., Ganey, J.L., Scott, P.E., and R. King. 2005. Prey ecology of Mexican spotted owls in pine–oak forests of northern Arizona. *The Journal of Wildlife Management* 69(2):618–629.

Borchers, D.L. and M.G. Efford. 2008. Spatially Explicit Maximum Likelihood Methods for Capture–Recapture Studies. *Biometrics* 64(2):377–385. https://doi.org/https://doi.org/10.1111/j.1541-0420.2007.00927.

Burnham, K.P. and D.R. Anderson. 2004. Multimodel Inference: Understanding AIC and BIC in Model Selection. *Sociological Methods & Research* 33(2):261–304. https://doi.org/10.1177/0049124104268644.

Burnham, K.P., Anderson, D.R., and K.P. Huyvaert. 2011. AIC model selection and multimodel inference in behavioral ecology: some background, observations, and comparisons. *Behavioral ecology and sociobiology* 65(1):23–35.

Caceres, N.C., Nápoli, R.P., and Hannibal, W. 2011. Differential trapping success for small mammals using pitfall and standard cage traps in a woodland savannah region of southwestern Brazil. 75(1):45–52. https://doi.org/doi:10.1515/mamm.2010.069.

Caughley, G. 1966. Mortality patterns in mammals. *Ecology* 47(6):906–918.

Cranford, J.A. 1977. Home Range and Habitat Utilization by Neotoma fuscipes as Determined by Radiotelemetry. Journal of Mammalogy 58 (2): 165–172. https://doi.org/10.2307/1379573. https://doi.org/10.2307/1379573.

Cranford, J.A. 1982. The Effect of Woodrat Houses on Population Density of Peromyscus. *Journal of Mammalogy* 63 (4): 663–666. https://doi.org/10.2307/1380275. http://www.jstor.org/stable/1380275.

du Preez, B.D., Loveridge, A.J., and D.W. Macdonald. 2014. To bait or not to bait: A comparison of camera-trapping methods for estimating leopard Panthera pardus density. *Biological Conservation* 176:153–161. https://doi.org/https://doi.org/10.1016/j.biocon.2014.05.021.

Efford, M.G., Dawson, D.K., and D.L. Borchers. 2009. Population density estimated from locations of individuals on a passive detector array. *Ecology* 90(10):2676–2682.

Efford, M.G. 2021. *secr*: Spatially explicit capture-recapture models version 4.4.7.

Ganey, J.L. 1992. Food habits of Mexican spotted owls in Arizona. *The Wilson Bulletin* 104(2):321–326.

Ganey, J.L., Kyle, S.C., Rawlinson, T.A., Apprill, D.L., and J.P. Ward Jr. 2014. Relative abundance of small mammals in nest core areas and burned wintering areas of Mexican Spotted Owls in the Sacramento Mountains, New Mexico. *The Wilson Journal of Ornithology* 126(1):47–52.

Gaukler, S.M., Murphy, S.M., Berryhill, J.T., Thompson, B.E., Sutter, B.J., and Hathcock, C.D. 2020. Investigating effects of soil chemicals on density of small mammal bioindicators using spatial capture-recapture models. PloS one 15(9):e0238870. https://doi.org/10.1371/journal.pone.0238870.

Gerber, B.D., and Parmenter, R.R. 2015. Spatial capture–recapture model performance with known small-mammal densities. *Ecological Applications* 25(3):695-–705. https://doi.org/https://doi.org/10.1890/14-0960.1.

Literature Cited

Gutierrez, R.J., A.B. Franklin, and W.S. Lahaye. 2020. Spotted Owl (*Strix occidentalis*), version 1.0. *In* Birds of the World (A. F. Poole and F. B. Gill, Editors). Cornell Lab of Ornithology, Ithaca, NY, USA. https://doi.org/10.2173/bow.spoowl.01

Hoffmann, J., Schirmer, A., and J.A. Eccard. 2019. Light pollution affects space use and interaction of two small mammal species irrespective of personality. *BMC Ecology* 19(1):26. https://doi.org/10.1186/s12898-019-0241-0.

Jensen, S.P. and P. Honess. 1995. The influence of moonlight on vegetation height preference and trappability of small mammals. *Mammalia* 59(1):35–42. https://doi.org/doi:10.1515/mamm.1995.59.1.35.

Lindstedt, S.L., Miller, B.J., and S.W. Buskirk. 1986. Home Range, Time, and Body Size in Mammals. *Ecology* 67(2):413–418.

Los Alamos National Laboratory (LANL). 1997. A checklist of mammals found at Los Alamos National Laboratory and surrounding areas. Los Alamos National Laboratory report LA-UR-97-4786.

Los Alamos National Laboratory (LANL). 2005. Small Mammal Sampling in Mortandad and Los Alamos Canyons, 2005. Los Alamos National Laboratory report LA-14301.

Los Alamos National Laboratory (LANL). 2006. Prey Remains Found in Pellets of Mexican Spotted Owls (Strix occidentalis lucida) from Los Alamos, New Mexico. Los Alamos National Laboratory report LA-UR-06-6757.

Los Alamos National Laboratory (LANL). 2017. Threatened and endangered species habitat management plan for Los Alamos National Laboratory. Los Alamos National Laboratory report LA-UR-17-29454.

Los Alamos National Laboratory (LANL). 2021. Status of Federally Listed Threatened and Endangered Species at Los Alamos National Laboratory. Los Alamos National Laboratory report LA-UR-21-30846.

Lynch, M.F., Fesnock, A. L., and Van Vuren, D. 1994. Home Range and Social Structure of the Dusky-Footed Woodrat (Neotoma fuscipes). *Northwestern Naturalist* 75(2):73–75. https://doi.org/10.2307/3536768. http://www.jstor.org/stable/3536768.

Murphy, S.M., Cox, J.J., Augustine, B.C., Hast, J.T., Guthrie, J.M., Wright, J., McDermott, J., Maehr, S.C., and J.H. Plaxico. 2016. Characterizing recolonization by a reintroduced bear population using genetic spatial capture–recapture. *Journal of Wildlife Management* 80(8):1390–1407.

Oksanen, J., Blanchet, F.G., Kindt, R., Legendre, P., Minchin, P.R., O'hara, R., Simpson, G.L., Solymos, P., Stevens, M.H.H., and H. Wagner. 2020. *vegan*: Community ecology package version 2.5-7.

Otis, D.L., Burnham, K.P., White, G.C., and D.R. Anderson. 1978. Statistical Inference from Capture Data on Closed Animal Populations. *Wildlife Monographs* (62):3–135.

R Development Core Team. 2021. R: A Language and Environment for Statistical Computing. R Foundation for Statistical Computing, Vienna, Austria.

Ribeiro, P.J., and P.J. Diggle. 2020. *geoR*: Analysis of geostatistical data version 1.8-1.

Royle, J.A., Chandler, R.B., Sollmann, R., and B. Gardner. 2014. *Spatial Capture-Recapture*. Wltham, MA: Elsevier.

Rstudio Team. 2020. RStudio: Integrated Development for R. Rstudio, PBC, Boston, MA.

Seamans, M.E. and R.J. Gutierrez. 1999. Diet composition and reproductive success of Mexican Spotted Owls. *Journal of Raptor Research* 33(2):143–148.

Literature Cited

Shannon, C.E. 1948. A mathematical theory of communication. *The Bell System Technical Journal* 27(3): 379–423. https://doi.org/10.1002/j.1538-7305.1948.tb01338.x.

Sikes, R.S., Bryan II, J.A., Byman, D., Danielson, B.J., Eggleston, J., Gannon, M.R., Gannon, W.L., Hale, D.H., Jesmer, B.R., Odell Hubbs, D.K., Olson, L.E., Stevens, R.D., Thompson, T.A., Timm, R.M., Trewhitt, S.A., and J.R. Willoughby. 2016. 2016 Guidelines of the American Society of Mammalogists for the use of wild mammals in research and education. *Journal of Mammalogy* 97(3):663–688. https://doi.org/10.1093/jmammal/gyw078.

U.S. Fish and Wildlife Service (USFWS). 1995. Recovery Plan for the Mexican Spotted Owl. U.S. Fish and Wildlife Service, Albuquerque, New Mexico.

U.S. Fish and Wildlife Service (USFWS). 2012. Recovery Plan for the Mexican Spotted Owl, First Revision. U.S. Fish and Wildlife Service, Albuquerque, New Mexico.

Vernes, K. 2003. Fine-scale habitat preferences and habitat partitioning by three mycophagous mammals in tropical wet sclerophyll forest, north-eastern Australia. *Austral Ecology* 28(5):471–479. https://doi.org/10.1046/j.1442-9993.2003.01303.

Ward, J.P Jr. and W.M. Block. 1995. Mexican Spotted Owl Prey Ecology. U.S. Department of Agriculture, Fish and Wildlife Service, Albuquerque, New Mexico.

Ward, J.P. Jr., Gutierrez, R.J., and B.R. Noon. 1998. Habitat selection by Northern Spotted Owls: The Consequences of prey selection and distribution. *The Condor* 100(1):79–92. https://doi.org/10.2307/1369899.

Willey, D.W. 2013. Diet of Mexican Spotted Owls in Utah and Arizona. *The Wilson Journal of Ornithology* 125(4):775–781. https://doi.org/10.1676/13-026.1.

Yunger, J.A., Meserve, P.L., and J.R. Gutierrez. 2002. Small-mammal foraging behavior: Mechanisms for coexistence and implication for population dynamics. *Ecological Monographs* 72(4):561–577.

Appendix

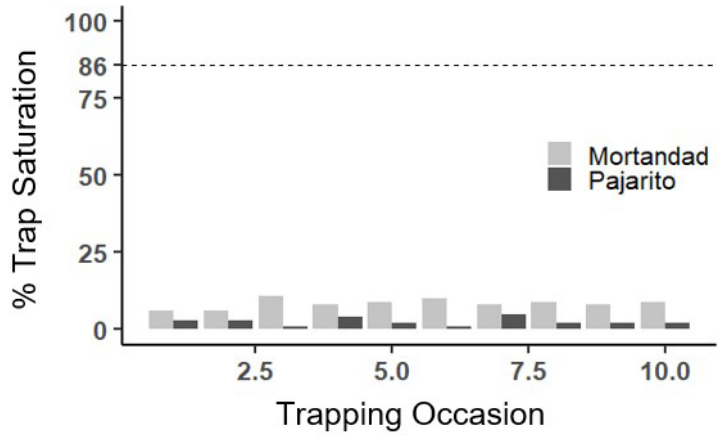

Figure A-1. Trap saturation (percent of traps occupied on each trapping occasion) by chronological trapping occasion for each trapping site. Notice all trap saturation values fall well below the 86% threshold advised in Royle et al. 2014 for modeling single-catch traps as multi-catch.

Table A-1. Model comparison for choice of detection functions (HF) and anisotropic transformation (presence of $\Phi(\sim 1)$) in the model column for each species and site with adequate encounter data ranked by Akaike's Information Criterion corrected for small sample size (AICC). Model formulas indicate parameter estimates for density in individuals per hectare (D), detection probability (g0), and spatial scale of detection (σ). The table reports number of parameters (K), AIC adjusted for small sample sizes (AICC), relative differences between model and highest ranked model AIC_C (ΔAIC_C), model weight (ω), and log likelihood of model (logLik).

Mortandad						
N. mexicana						
Model	HF	K	AIC_C	ΔAIC_C	ω	logLik
$D(\sim 1)\ g_0(\sim 1)\ \sigma(\sim 1)\ \Phi(\sim 1)$	EX	5	450.0	0.00	0.87	–216.7
$D(\sim 1)\ g_0(\sim 1)\ \sigma(\sim 1)$	EX	4	453.8	3.75	0.13	–220.9
$D(\sim 1)\ g_0(\sim 1)\ \sigma(\sim 1)\ \Phi(\sim 1)$	HN	5	469.7	19.7	0.00	–226.5
$D(\sim 1)\ g_0(\sim 1)\ \sigma(\sim 1)$	HN	4	471.9	21.9	0.00	–230.0
P. boylii						
Model	*HF*	K	AIC_C	ΔAIC_C	ω	logLik
$D(\sim 1)\ g_0(\sim 1)\ \sigma(\sim 1)\ \Phi(\sim 1)$	HN	5	391.1	0.00	0.51	–186.8
$D(\sim 1)\ g_0(\sim 1)\ \sigma(\sim 1)\ \Phi(\sim 1)$	EX	5	391.9	0.83	0.34	–187.2
$D(\sim 1)\ g_0(\sim 1)\ \sigma(\sim 1)$	EX	4	394.9	3.81	0.08	–191.2
$D(\sim 1)\ g_0(\sim 1)\ \sigma(\sim 1)$	HN	4	395.1	4.00	0.07	–191.3
Pajarito						
N. mexicana						
Model	*HF*	K	AIC_C	ΔAIC_C	ω	logLik
$D(\sim 1)\ g_0(\sim 1)\ \sigma(\sim 1)$	EX	4	251.9	0.00	0.71	–115.3
$D(\sim 1)\ g_0(\sim 1)\ \sigma(\sim 1)$	HN	4	253.7	1.83	0.29	–116.2
$D(\sim 1)\ g_0(\sim 1)\ \sigma(\sim 1)\ \Phi(\sim 1)$	EX	5	262.4	10.5	0.00	–111.2
$D(\sim 1)\ g_0(\sim 1)\ \sigma(\sim 1)\ \Phi(\sim 1)$	HN	5	265.9	14.0	0.00	–112.9

Table A-2. Pooled model comparison for choice of detection functions (HF) and anisotropic transformation (presence of $\Phi(\sim 1)$) in the model column for each site, combining all species, ranked by Akaike's Information Criterion corrected for small sample size (AICC). Model formulas indicate parameter estimates for density in individuals per hectare (D), detection probability (g0), and spatial scale of detection (σ). Table reports number of parameters (K), AIC adjusted for small sample sizes (AICC), relative differences between model and highest ranked model AIC_C (ΔAIC_C), model weight (ω), and log likelihood of model (logLik).

Mortandad						
Model	HF	K	AIC_C	ΔAIC_C	ω	logLik
$D(\sim 1)\ g_0(\sim 1)\ \sigma(\sim 1)\ \Phi(\sim 1)$	EX	5	800.0	0.00	1.00	–393.7
$D(\sim 1)\ g_0(\sim 1)\ \sigma(\sim 1)\ \Phi(\sim 1)$	HN	5	817.3	17.3	0.00	–402.3
$D(\sim 1)\ g_0(\sim 1)\ \sigma(\sim 1)$	EX	4	817.3	17.3	0.00	–403.8
$D(\sim 1)\ g_0(\sim 1)\ \sigma(\sim 1)$	HN	4	834.7	34.6	0.00	–412.5
Pajarito						
Model	HF	K	AIC_C	ΔAIC_C	ω	logLik
$D(\sim 1)\ g_0(\sim 1)\ \sigma(\sim 1)\ \Phi(\sim 1)$	EX	5	312.8	0.00	0.46	–146.4
$D(\sim 1)\ g_0(\sim 1)\ \sigma(\sim 1)$	HN	4	312.9	0.10	0.44	–149.6
$D(\sim 1)\ g_0(\sim 1)\ \sigma(\sim 1)$	HN	4	316.5	3.64	0.07	–151.4
$D(\sim 1)\ g_0(\sim 1)\ \sigma(\sim 1)\ \Phi(\sim 1)$	EX	5	318.1	5.25	0.03	–149.0

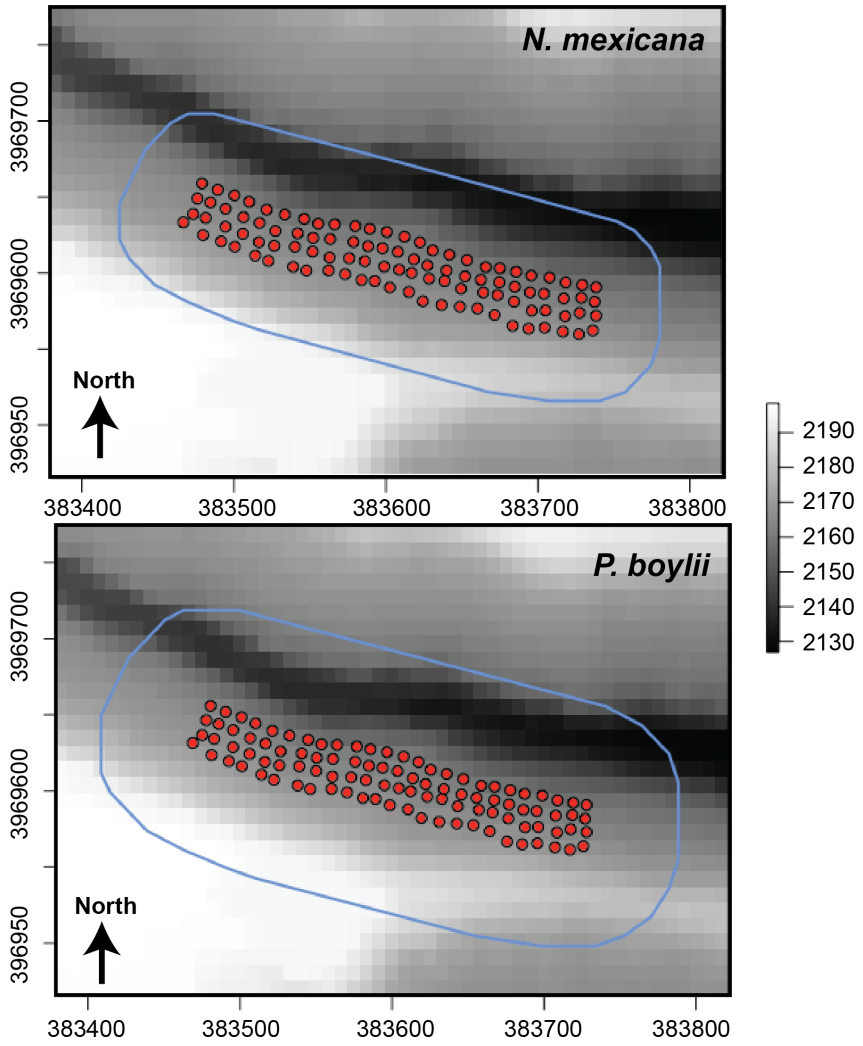

Figure A-2. State space for Mexican woodrat SCR models (top) and brush mouse (bottom) at the Pajarito trapping site. Blue line delineates state space–based detection probability attenuation from top model(s). Red points indicate trap positions in state space. Background is shaded by elevation in meters (see scale bar). Axes show coordinates for UTM zone 13 North.

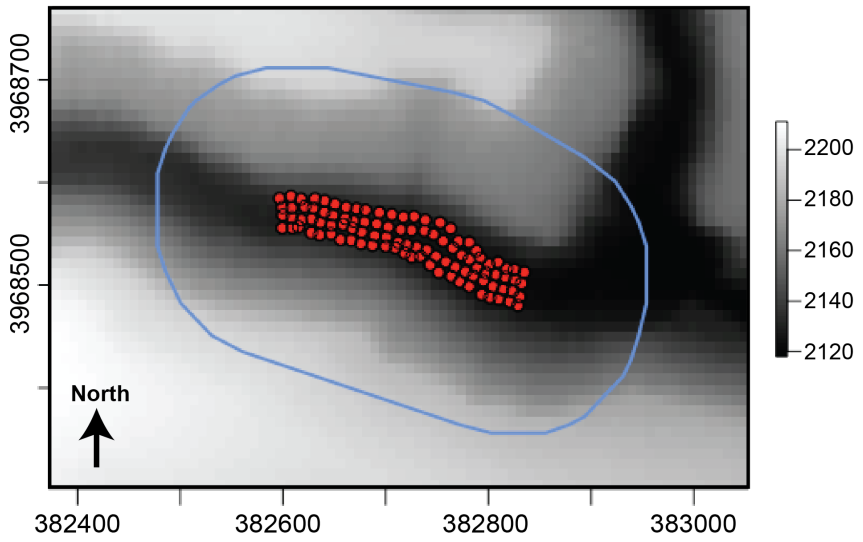

Figure A-3. State space for Mexican woodrat SCR models at the Pajarito trapping site. Blue line delineates state space–based detection probability attenuation from top model(s). Red points indicate trap positions in state space. Background is shaded by elevation in meters (see scale bar). Axes show coordinates for UTM zone 13 North.

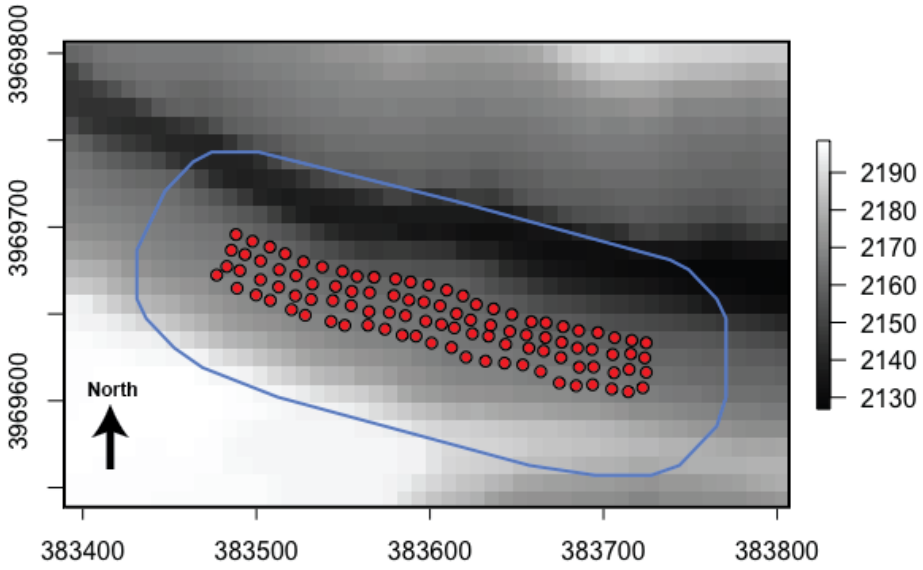

Figure A-4. State space for pooled small mammal SCR models at the Mortandad Bench trapping site. Blue line delineates state space–based detection probability attenuation from top model(s). Red points indicate trap positions in state space. Background is shaded by elevation in meters (see scale bar). Axes show coordinates for UTM zone 13 North.

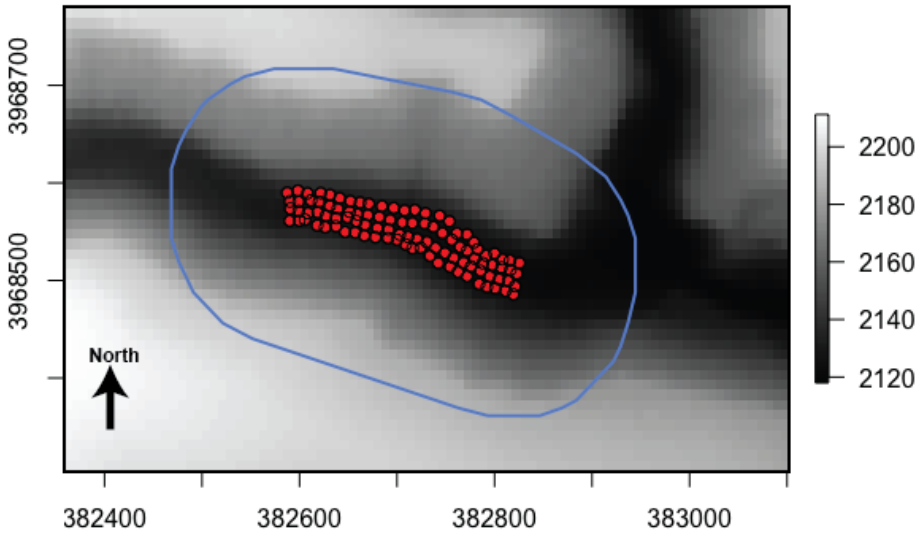

Figure A-5. State space for pooled small mammal SCR models at the Pajarito trapping site. Blue line delineates state space–based on detection probability attenuation from top ranked model(s). Red points indicate trap positions in state space. Background shaded by elevation in meters (see scale bar). Axes show coordinates for UTM zone 13 North.

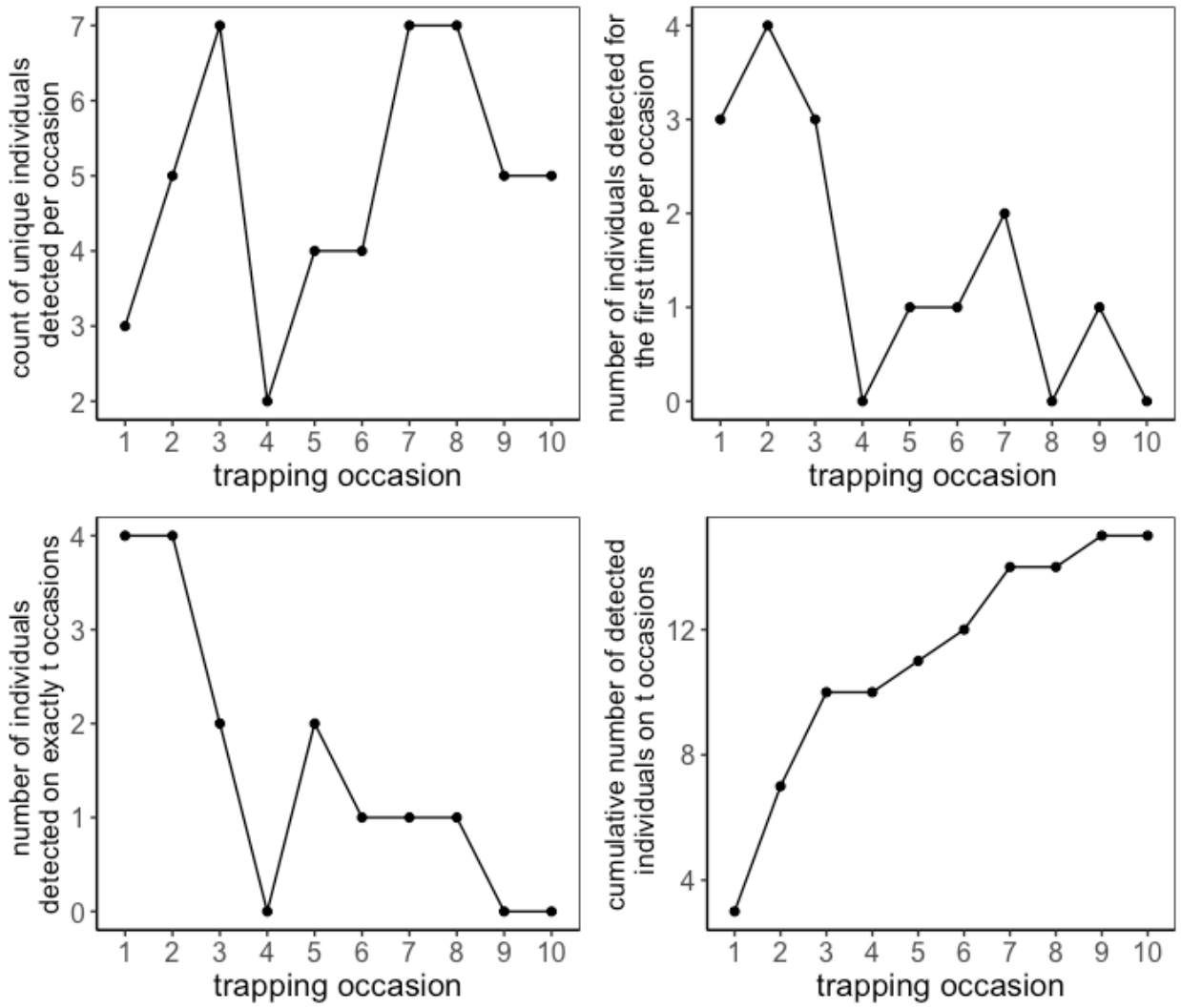

Figure A-6. Trapping history of Mexican woodrat at the Mortandad trapping site. Top left panel shows number of unique individuals captured each day traps were operational. Top right panel shows number of individuals captured for the first time on each day traps were operational. Bottom left panel shows number of individuals captured on exactly t occasions (i.e., we detected no individuals on exactly four occasions). Bottom right panel shows cumulative number of individuals after t trapping occasions.

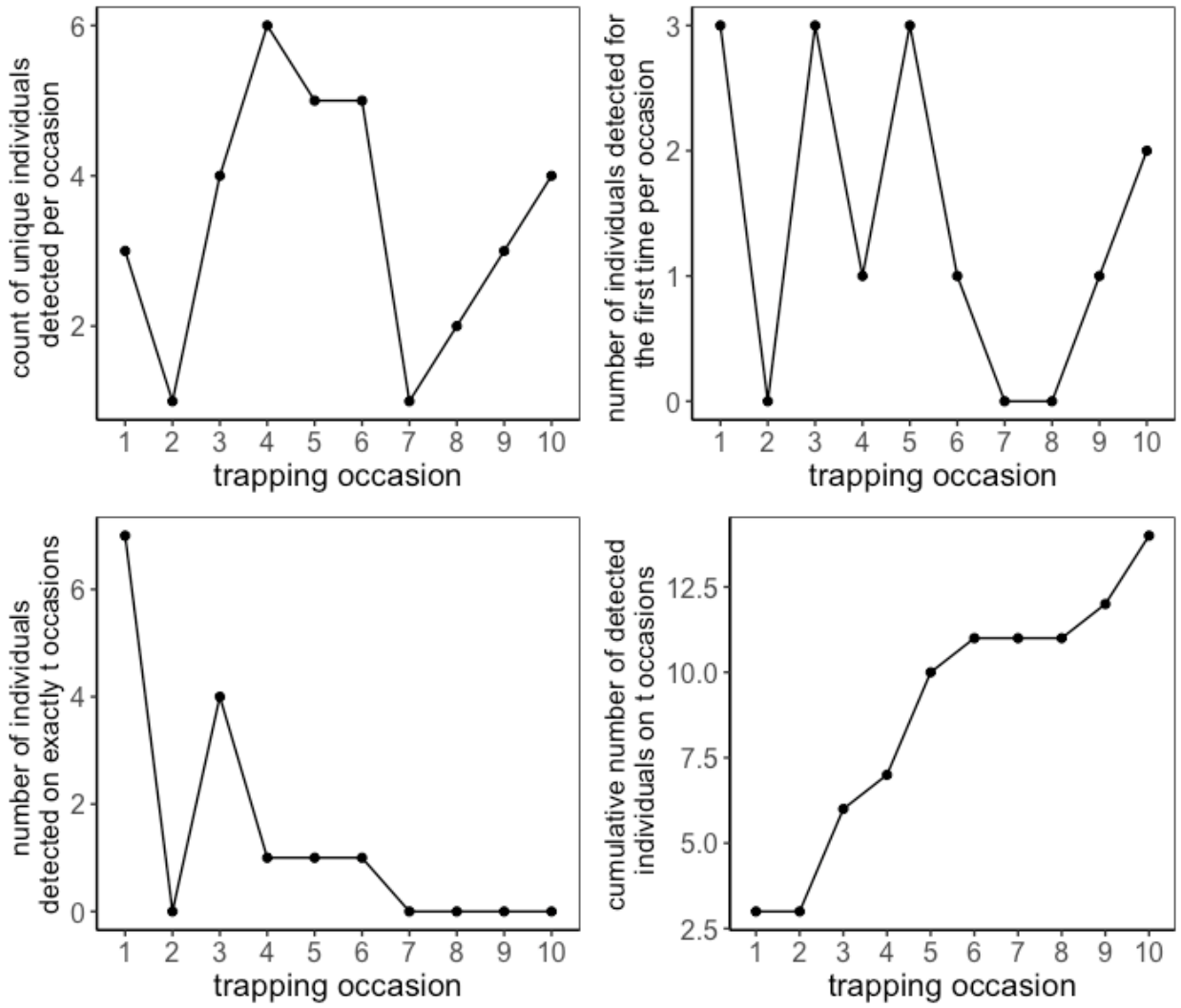

Figure A-7. Trapping history of brush mouse at the Mortandad trapping site. Top left panel shows number of unique individuals captured each day traps were operational. Top right panel shows number of individuals captured for the first time on each day traps were operational. Bottom left panel shows number of individuals captured on exactly t occasions (i.e., we detected no individuals on exactly two occasions). Bottom right panel shows cumulative number of individuals after t trapping occasions.

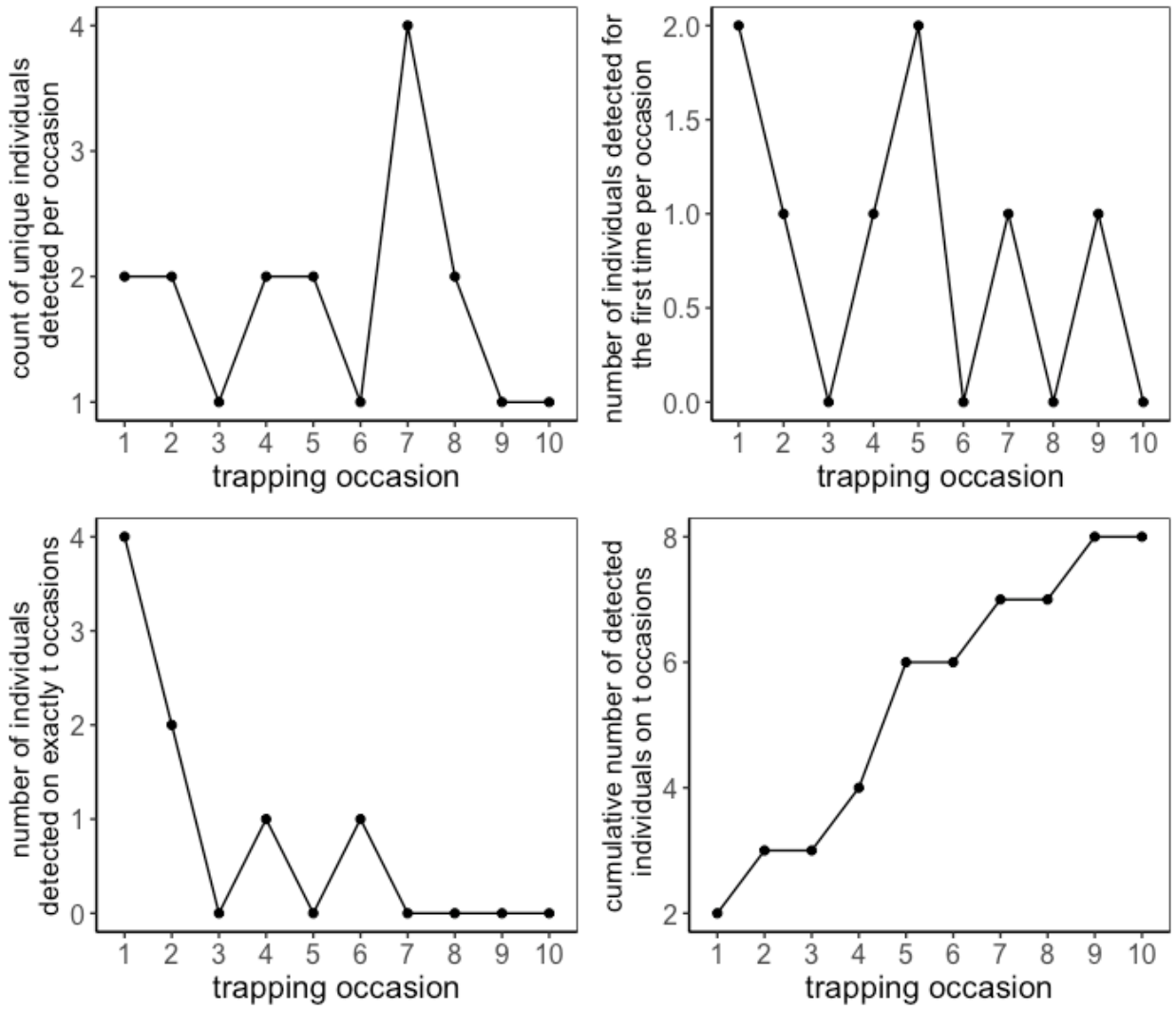

Figure A-8. Trapping history of Mexican woodrat at the Pajarito trapping site. Top left panel shows number of unique individuals captured each day traps were operational. Top right panel shows number of individuals captured for the first time on each day traps were operational. Bottom left panel shows number of individuals captured on exactly t occasions (i.e., we detected no individuals on exactly five occasions). Bottom right panel shows cumulative number of individuals after t trapping occasions.

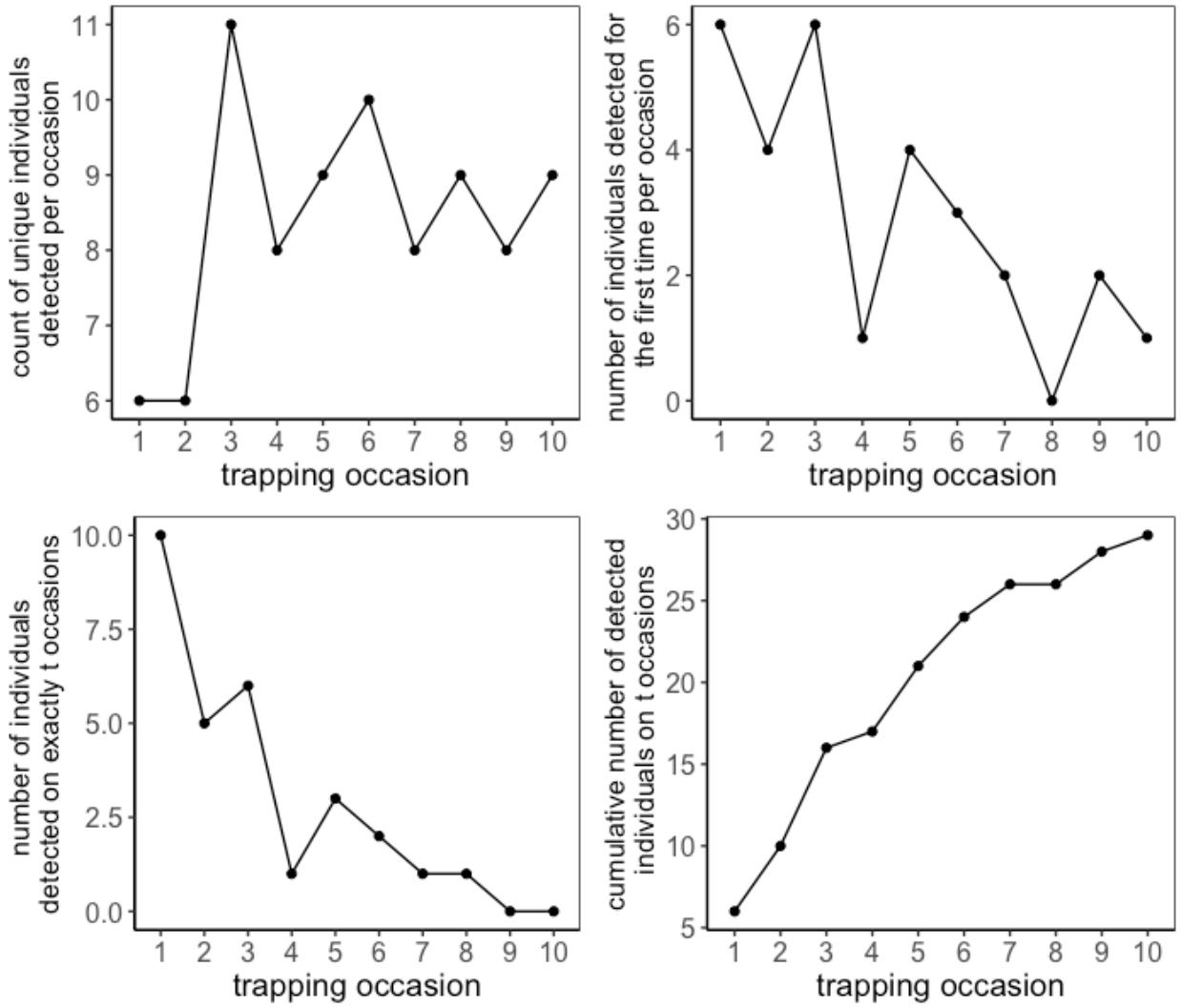

Figure A-9. Trapping history of small mammals at the Mortandad trapping site. Top left panel shows number of unique individuals captured each day traps were operational. Top right panel shows number of individuals captured for the first time on each day traps were operational. Bottom left panel shows number of individuals captured on exactly t occasions (i.e., we detected no individuals on exactly five occasions). Bottom right panel shows cumulative number of individuals after t trapping occasions.

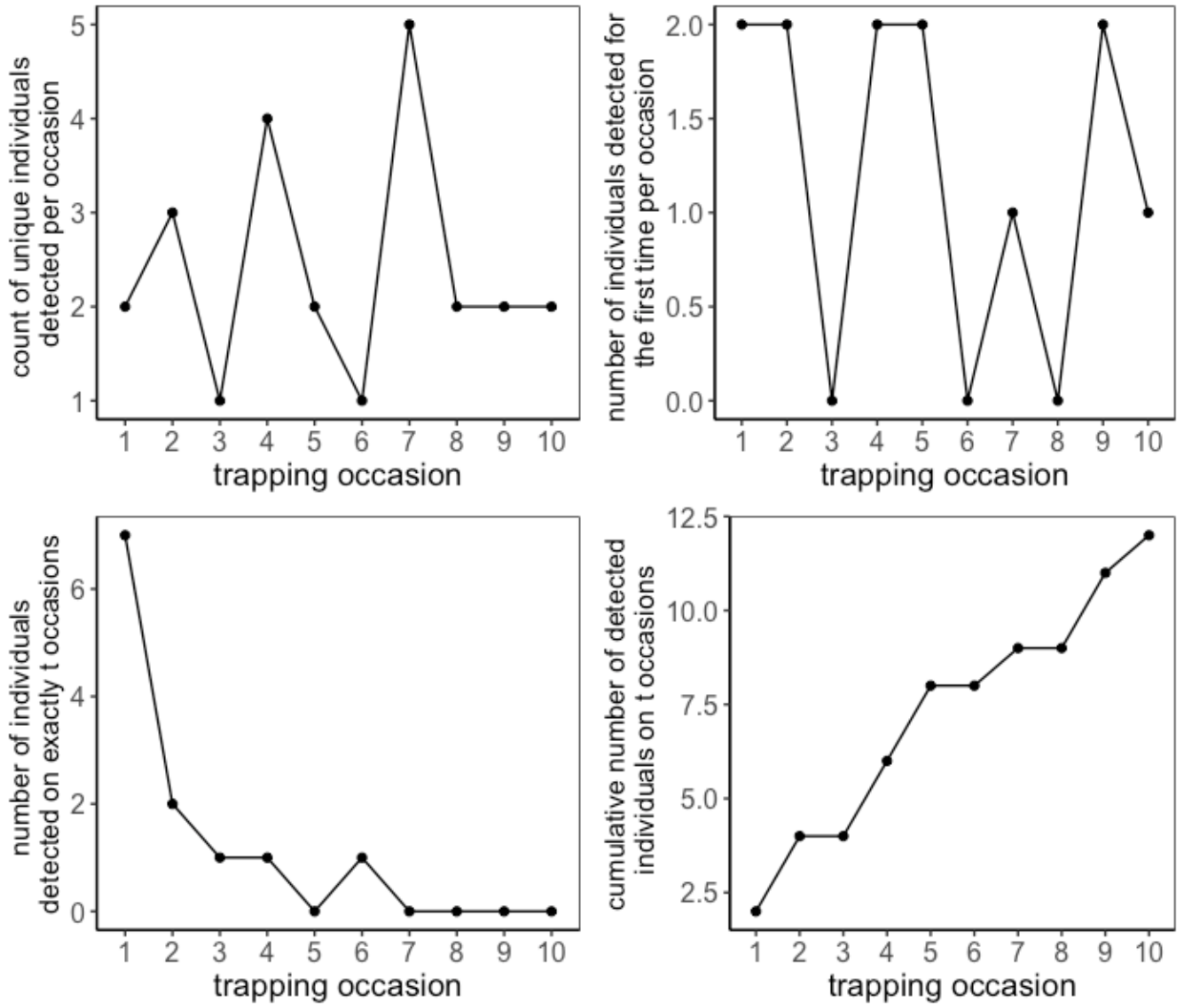

Figure A-10. Trapping history of small mammals at the Pajarito trapping site. Top left panel shows number of unique individuals captured each day traps were operational. Top right panel shows number of individuals captured for the first time on each day traps were operational. Bottom left panel shows number of individuals captured on exactly t occasions (i.e., we detected no individuals on exactly five occasions). Bottom right panel shows cumulative number of individuals after t trapping occasions.

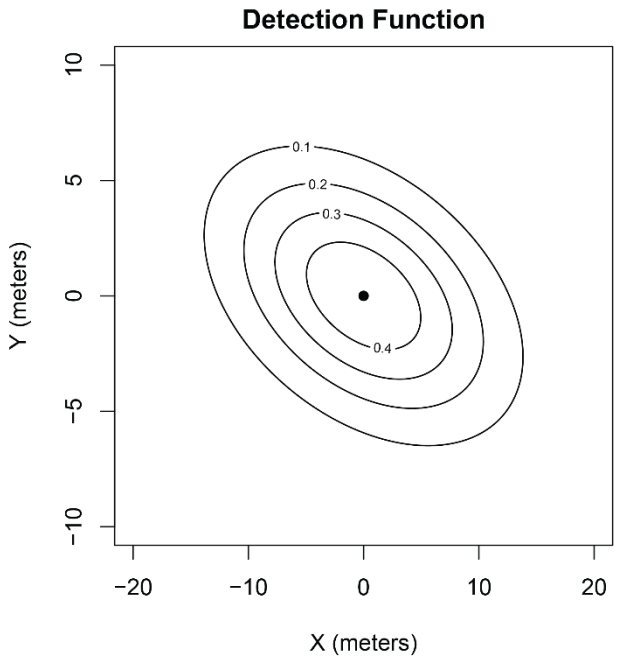

Figure A-11. Anisotropic transformation of negative exponential detection function for Mexican woodrat at Mortandad trapping site.

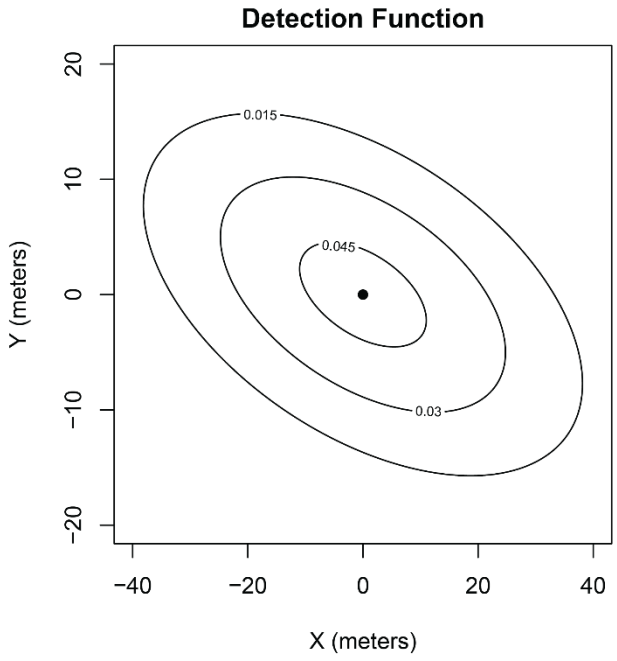

Figure A-12. Anisotropic transformation of negative exponential detection function for brush mouse at Mortandad trapping site.

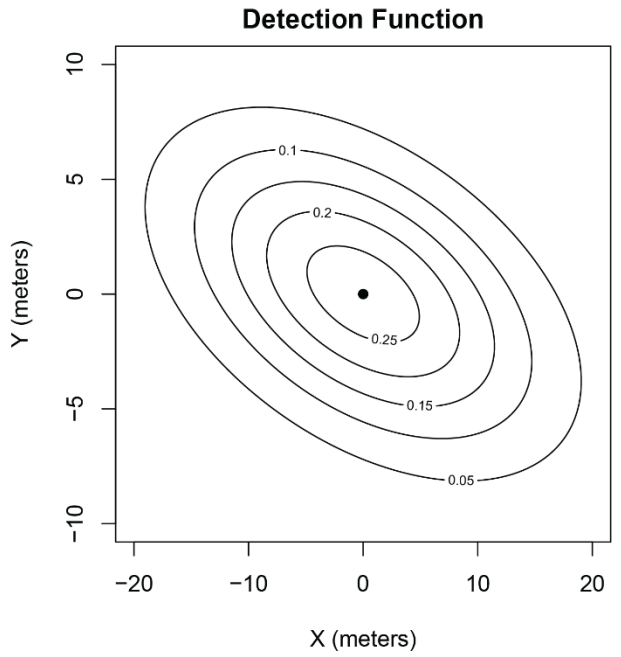

Figure A-13. Anisotropic transformation of negative exponential detection function for small mammals at Mortandad trapping site.

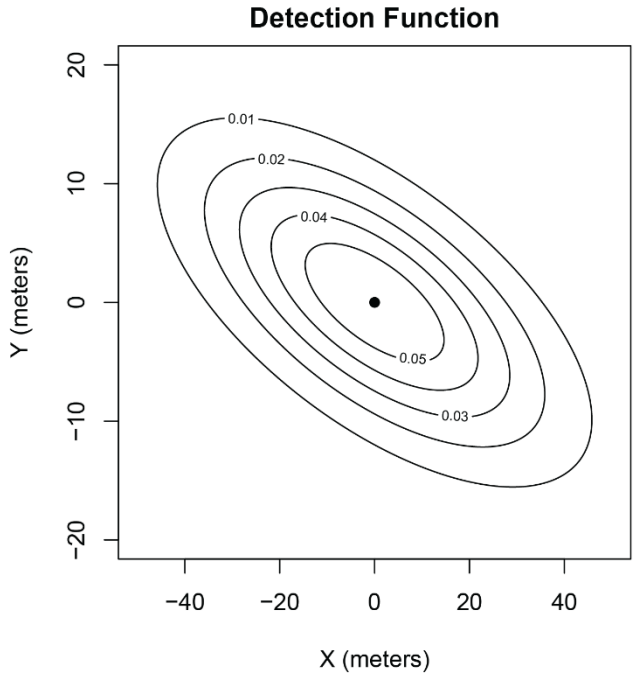

Figure A-14. Anisotropic transformation of negative exponential detection function for small mammals at Pajarito trapping site.